

Article

Chemical Investigation of the Indonesian Tunicate *Polycarpa aurata* and Evaluation of the Effects Against *Schistosoma mansoni* of the Novel Alkaloids Polyaurines A and B

Marcello Casertano ¹, Concetta Imperatore ¹, Paolo Luciano ¹, Anna Aiello ¹,
Masteria Yunovilsa Putra ² , Roberto Gimmelli ³, Giovina Ruberti ³  and
Marialuisa Menna ^{1,*} 

¹ The NeaNat Group, Department of Pharmacy, University of Naples “Federico II”, Via D. Montesano 49, 80131 Napoli, Italy; marcello.casertano@unina.it (M.C.); cimperat@unina.it (C.I.); pluciano@unina.it (P.L.); aiello@unina.it (A.A.)

² Research Center for Oceanography, Indonesian Institute of Sciences, Jl Pasir Putih Raya 1, DKI Jakarta 14430, Indonesia; mast001@lipi.go.id

³ Institute of Cell Biology and Neurobiology, National Research Council, Campus A. Buzzati-Traverso, Via E. Ramarini, 32, 00015 Monterotondo (Roma), Italy; roberto.gimmelli@ibcn.cnr.it (R.G.); giovina.ruberti@cnr.it (G.R.)

* Correspondence: mlmenna@unina.it; Tel.: +39-081-678-518

Received: 15 April 2019; Accepted: 7 May 2019; Published: 10 May 2019



Abstract: A deep study of the metabolic content of the tunicate *Polycarpa aurata*, collected from Indonesian coast, afforded the isolation of two novel alkaloids, polyaurines A (**1**) and B (**2**), along with two new *p*-substituted benzoyl derivatives (**3** and **4**) and four known compounds (**5–8**). The structural elucidation of the new secondary metabolites was assigned by 1D, 2D NMR, and HRESIMS techniques. Computational studies resulted a useful tool to unambiguously determine in polyaurine B the presence of rarely found 1,2,4-thiadiazole ring. The effects of polyaurines A and B on mammalian cells growth and on the viability of different blood-dwelling *Schistosoma mansoni* (phylum: Platyhelminthes) stages, as well as egg production, were evaluated. Both compounds resulted not cytotoxic; interestingly some of the eggs produced by polyaurine A-treated adult pairs *in vitro* are smaller, deformed, and/or fragmented; therefore, polyaurine A could represent an interesting bioactive natural molecule to be further investigated.

Keywords: natural products; ascidians; *Polycarpa aurata*; 1,2,4-thiadiazole alkaloids; *Schistoma mansoni*

1. Introduction

The solitary ascidian *Polycarpa aurata* (Quoi and Gaimard, 1834), a common constituent of the benthic invertebrate community of Indo-Pacific coral reefs has proved to be an extremely rich source of chemo diversity, especially of unique alkaloid-type structures. Typically, the heterocycle parts commonly found in the structures of natural products contain one or two heteroatoms, most frequently nitrogen and/or oxygen and occasionally sulfur [1]. Indeed, many alkaloids with rare sulfur-containing functional groups and/or featuring different heterocycle portion have been isolated from this marine invertebrate. Examples are the dimeric disulfide alkaloid polycarpine and its derivatives [2], the polycarpamines A–E [3], the 2-aminoimidazole polycarpaurines A–C [4], the indole alkaloid *N,N*-didesmethylgrossularine-1 [2], and the unique 1,2,4-thiadiazole alkaloids polycarpathiamines A and B [5]. In addition to these very unusual alkaloids, a series of both nitrogen-containing and

non-nitrogenous benzoyl derivatives were also isolated from this ascidian species [6]. Most of these compounds exhibited various biological activities, such as antifungal [3], cytotoxic [2,4,7,8], pro-apoptotic [9], and inosine monophosphate dehydrogenase (IMPDH) inhibiting activities [2]. The extremely high chemical diversity of *P. aurata* and observation that different collections of this organism yielded different metabolites patterns suggested that the ascidian may not be the real producer of these unique compounds and that their bioproduction could involve associated microorganisms or the planktonic biomass [3].

In the frame of our continuing search for novel bioactive compounds from marine ascidians, we have investigated a sample of *P. aurata* collected along the coast of Siladen (Indonesia); the chemical analysis of the methanol extract of this organism afforded four new metabolites (compounds 1–4, Figure 1), along with four known compounds (5–8, Figure 1) previously reported from *P. aurata* and other *Polycarpa* species. Compounds 5–8 were identified as polycarpathiamine B (5) [5], 4-methoxy-4-(4-methoxyphenyl)-1-methyl-5-thioxoimidazolidin-2-one (6) [2,7], methyl 2-(4-methoxyphenyl)-2-oxoacetate (7) [6], and 2-(4-methoxyphenyl)-*N*-methyl-2-oxoacetamide (8) [6] by comparison of their spectral data with those reported in the literature. The structures of the two new benzoyl derivatives ethyl 2-(4-methoxyphenyl)-2-oxoacetate (3) and methyl 2-(4-hydroxyphenyl)-2-oxoacetate (4) were also easily assigned based on their spectral properties compared to those of the strictly related known compounds 7 and 8 [6].

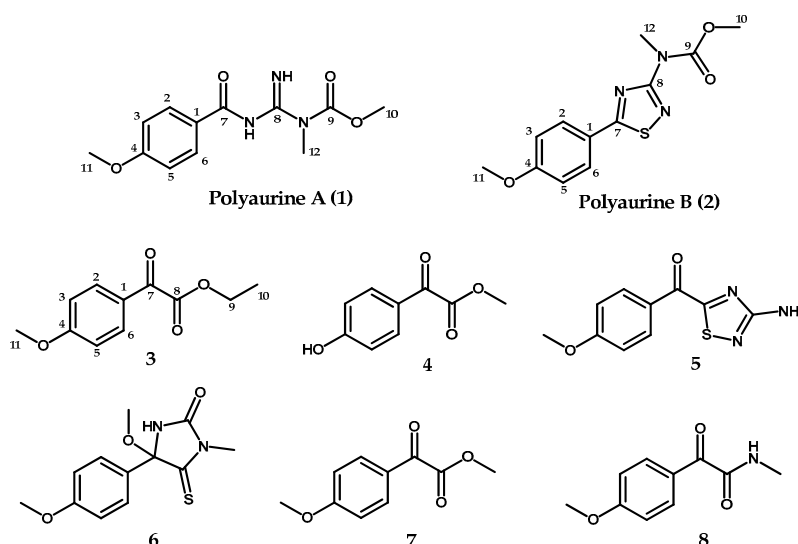


Figure 1. Structures of compounds 1–8.

We describe herein the isolation and structure elucidation of the two novel alkaloids 1 and 2 that we named polyaurines A and B, respectively. Notably, the structure of polyaurine B contains the “heteroatom-rich” 1,2,4-thiadiazole nucleus, which is really uncommon in natural products [5]; compound 2 represents, to our knowledge, the first example of a 3-(*N*-methyl-methylcarbamate) substituted 1,2,4-thiadiazole alkaloid.

Despite the small amounts of compounds that we succeeded in obtaining from the extraction of the ascidian sample, we have investigated the effects of the two novel alkaloids, 1 and 2, on the viability of *Schistosoma mansoni* larval and adult stages and egg production. Schistosomiasis is one of the most important parasitic diseases, with more than 200 million people infected globally by the Platyhelminthes of the genus *Schistosoma*. The parasite has a complex life cycle that includes several morphological phenotypes in the intermediate fresh-water snail host (*Biomphalaria* spp.) and in the mammalian definitive host. Adult *S. mansoni* worms live predominantly in the small inferior mesenteric blood vessels where the mated females release hundreds of eggs daily. Excretion of eggs within the fecal material maintains the parasites life-cycle. The eggs trapped in the liver evoke inflammation

and host-immune reactions leading to the formation of granuloma around the eggs and progressive organ damage and pathology [10,11]. Here, we show that some of the eggs produced by polyaurine A-treated adult pairs in vitro are smaller, deformed, and/or fragmented. Importantly, the polyaurine A (1) is not cytotoxic against mammalian cells; therefore, it could represent an interesting bioactive natural molecule to be further investigated.

2. Results

2.1. Isolation and Structure Elucidation of Compounds 1–2

Several fresh specimens of *P. aurata* were extracted with methanol and, then, with chloroform. Solvent partitioning of the combined extracts yielded a lipid soluble portion, which was fractionated by silica gel medium pressure chromatography. TLC and ^1H NMR guided separations and purifications by HPLC of the obtained fractions afforded compounds 1–8 in the pure state.

The HRESIMS of polyaurine A (1) showed peaks at m/z 266.1129 $[\text{M} + \text{H}]^+$ and 288.0948 $[\text{M} + \text{Na}]^+$ suggesting the molecular formula $\text{C}_{12}\text{H}_{16}\text{N}_3\text{O}_4$ with seven degrees of unsaturation. The ^1H and ^{13}C NMR data obtained for 1 and assigned through 2D NMR experiments (Table 1) evidenced the presence of a *p*-methoxyphenyl unit. In particular, the deshielding of two aromatic protons at δ_{H} 8.17 (2H, d, $J = 8.2$ Hz, H-2/6) and δ_{H} 6.89 (2H, d, $J = 8.2$ Hz, H-3/5) suggested the presence of a *para* oxygenated benzoyl system. Four carbon resonances, two protonated (δ_{C} 131.1 (C-2 and C-6) and 113.0 (C-3 and C-5)) and two unprotonated (δ_{C} 162.4 (C4) and 130.7 (C-1)), were assigned by HSQC and HMBC experiments (Table 1), to this aromatic moiety. The presence of a methoxy-functionality was inferred by the proton and carbon resonances at δ_{H} 3.84 (3H, s, Me-11) and δ_{C} 55.2 (C-11), respectively. HMBC correlations between these methoxyl protons and both the aromatic quaternary carbon at δ_{C} 162.4 (C-4) and the carbons at δ_{C} 113.0 (C-3/5) allowed to link this group at C-4. A 4-methoxybenzoyl unit was thus evident from the fragment peak at $m/z = 135$ in the MS/MS spectrum of 1 and from the HMBC correlation of the aromatic proton signals at δ_{H} 8.17 (H-2/6) with the carbonyl resonance at δ_{C} 177.9. This unit accounted for five of the seven degrees of unsaturation suggested by the molecular formula of 1.

Table 1. ^1H (700 MHz) and ^{13}C NMR (125 MHz) spectroscopic data ^a of polyaurines A (1) and B (2) in CDCl_3 .

| Pos | 1 ^a | | 2 ^a | |
|-----|---------------------|---------------------------------------|---------------------|---------------------------------------|
| | δ_{C} | δ_{H} (mult, J in Hz) | δ_{C} | δ_{H} (mult, J in Hz) |
| 1 | 130.7 | - | 123.2 | - |
| 2 | 131.1 | 8.17 (d, $J = 8.2$ Hz) | 128.9 | 7.88 (d, $J = 7.9$ Hz) |
| 3 | 113.0 | 6.89 (d, $J = 8.2$ Hz) | 114.7 | 6.96 (d, $J = 7.9$ Hz) |
| 4 | 162.4 | - | 162.7 | - |
| 5 | 113.0 | 6.89 (d, $J = 8.2$ Hz) | 114.7 | 6.96 (d, $J = 7.9$ Hz) |
| 6 | 131.1 | 8.17 (d, $J = 8.2$ Hz) | 128.9 | 7.88 (d, $J = 7.9$ Hz) |
| 7 | 177.9 | - | 187.1 | - |
| 8 | 159.8 | - | 165.8 | - |
| 9 | 156.7 | - | 154.9 | - |
| 10 | 53.8 | 3.86 (s) | 53.6 | 3.85 (s) |
| 11 | 55.2 | 3.84 (s) | 55.5 | 3.87 (s) |
| 12 | 32.3 | 3.52 (s) | 36.1 | 3.54 (s) |
| -NH | - | 9.28 (br. s); 10.58 (br. s) | - | - |

^a ^1H NMR and ^{13}C NMR shifts are referenced to CDCl_3 ($\delta_{\text{H}} = 7.26$ ppm and $\delta_{\text{C}} = 77.0$ ppm). The proton and carbon resonances were assigned by HSQC and HMBC experiments.

Additional features of the proton spectrum of 1 were two downfield signals at δ_{H} 9.28 (1H, br.s, NH) and δ_{H} 10.58 (1H, br.s, NH), as well as two methyl singlets at δ_{H} 3.86 (3H, s, Me-10) and 3.52 (3H, s, Me-12). The methyl signals could be assigned, based on their chemical shift values and both HSQC and HMBC correlations, to a nitrogen linked methyl group ($\delta_{\text{C}} = 32.3$) and to a methoxyl group

(δ_C 53.8), respectively. Two unprotonated sp^2 carbon resonances remained in the ^{13}C NMR spectrum of **1**, at δ_C 159.8 and 156.7. According to the molecular formula of **1** and based on the whole series of the HMBC correlations (Figure 2), a methyl-guanidine unit and a carbamate function were identified. Key correlations were those between the *N*-linked methyl group (Me-12, δ_H 3.52) and both the sp^2 carbon resonance at δ_C 159.8 and 156.7, the latter being correlated to the methoxyl group resonating at δ_H 3.86 (Me-10). Therefore, compound (**1**) was identified as depicted in Figure 2 and was named polyaurine A.

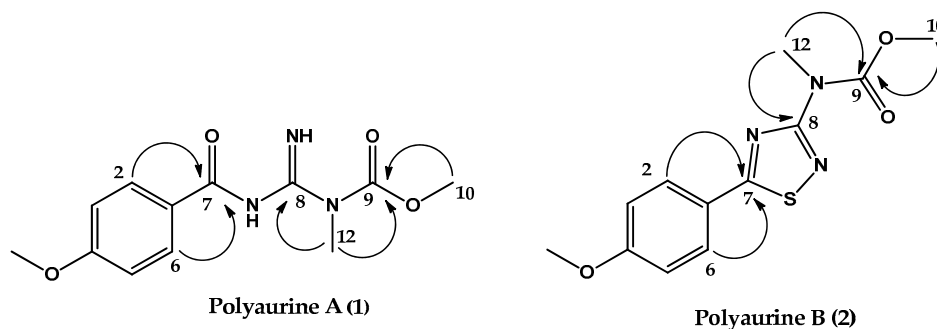


Figure 2. Key HMBC correlations of compounds **1** and **2**.

Polyaurine B (**2**) had the molecular formula $C_{12}H_{13}N_3O_3S$, as deduced from the HRESIMS spectrum (positive ion mode), which showed pseudomolecular ion peaks at m/z 280.0741 $[M + H]^+$ and m/z 302.0558 $[M + Na]^+$. The molecular formula indicated eight degrees of unsaturation, one more than polyaurine A. An extensive NMR analysis conducted on the molecule allowed the initial identification of three subunits in the structure (subunits A–C, Figure 3) that were subsequently connected through further HMBC experiments.

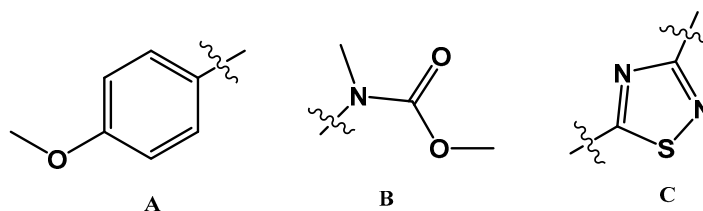


Figure 3. Subunits A–C of the structure of **2**.

The presence of the *p*-methoxyphenyl group (subunit A, Figure 3), which also appears in the structure of polyaurine A (**1**), was deduced from the aromatic methine resonances present in the 1H and ^{13}C NMR spectra ($CDCl_3$) [δ_H 7.88 (2H, d, $J = 7.9$ Hz, H-2/6); δ_H 6.96 (2H, d, $J = 7.9$ Hz, H-3/5); δ_C 128.9 (C-2 and C-6), δ_C 114.7 (C-3 and C-5)], the methoxyl signal at δ_H 3.87 (Me-11), and the unprotonated carbon signals at δ_C 162.7 (C4), 123.2 (C-1), and 55.5 (C-11), which were assigned to this aromatic system on the basis of two-dimensional HSQC and HMBC experiments (see Table 1). The latter experiment also showed that the methoxyl protons at δ_H 3.87 were correlated with both the quaternary carbon signal at δ_C 162.7 (C-4) and the methine signal at δ_C 114.7 (C-3/5). The remaining signals in the 1H NMR spectrum of **2** were two additional methyl singlets at δ_H 3.54 (3H, Me-12) and 3.85 (3H, Me-10); the relevant carbons, identified by the HSQC experiment, were at δ_C 36.1 and 53.6, respectively. These proton and carbon resonances were reasonably ascribed to an *N*-linked methyl and a methoxyl group, respectively. Both singlets at δ_H 3.54 and 3.85 were correlated in the HMBC spectrum to the quaternary sp^2 carbon resonance at δ_C 154.9. Based on these data, the *N*-methyl-methylcarbamate functionality (subunit B, Figure 3) was identified in **2**.

According to the molecular formula assigned to **2** by mass spectrometric analysis, one sulfur, two carbon, and two nitrogen atoms still remained to be placed in the molecule; moreover, three degrees of unsaturation had to be satisfied and only two quaternary sp^2 carbon signals, at δ_C 187.1 and

165.8, remained to be assigned. Thus, we hypothesized the third structural subunit in the molecule of compound **2** to be a 1,2,4-thiadiazole ring (subunit C, Figure 3), the only thiadiazole regioisomer known to occur naturally [1] and already found in the structure of polycarpathamines previously discovered from *P. aurata* [5]. Comparison of the chemical shift values of compound **2**, and precisely evaluation at δ_C values of the two carbons assigned to the heterocyclic ring, with those reported in the literature for both natural [5,12–14] and synthetic 1,2,4-thiadiazole alkaloids [14–17] allowed to substantiate this assumption.

The three identified structural subunits A–C were finally connected on the basis of key correlations observed in the HMBC spectrum. In detail, a correlation was observed between the aromatic proton signal at δ_H 7.88 (H-2/6) and the carbon signal at δ_C 187.1, relative to the carbon between the atoms of nitrogen and sulfur of the thiadiazole ring (C-7), whereas the protons of the *N*-linked group of subunit B (δ_H 3.54) showed a correlation with the remaining carbon of the subunit C resonating at δ_C 165.8. All these data allowed to propose the structure shown in Figure 2 for compound **2**, which is named polyaurine B.

The first reported example of a natural product containing the 1,2,4-thiadiazole heterocyclic moiety has been the alkaloid dendrodoine, isolated from the marine ascidian *Dendrodoa grossularia* (Styelidae) [12]. This compound has been the only example until 2012, when a pair of enantiomeric indole alkaloids containing the 1,2,4-thiadiazole unit were isolated from the plant *Isatis indigotica* [13]. The 3-amino substituted 1,2,4-thiadiazole alkaloids polycarpathamines have been isolated in 2013 from a marine ascidian [5], and, recently, the 1,2,4-thiadiazole alkaloid penicilliumthiamine B has been isolated from the fungus *Penicillium oxalicum* [14].

2.2. Validation of the Polyaurine B (2) Structure by Theoretical QM Calculations

To unequivocally prove the existence of the unusual 1,2,4-thiadiazole heterocyclic ring, structure elucidation of these compounds has been confirmed by synthesis [14–17] with respect of many spectroscopic evidences as well as biogenetic considerations. Instead, we obtained further support to the methyl 5-(4-methoxyphenyl)-1,2,4-thiadiazol-3-yl(methyl)carbamate structure proposed for polyaurine B, through the quantum mechanical calculation of its ^{13}C NMR chemical shifts profile and application of DP4+ statistical analysis. This approach, relying on the use of QM calculated NMR parameters profiles combined with refined data processed by appropriate “computational toolboxes,” is becoming increasingly important as a valuable theoretical supplement to the experimental spectroscopic, both chiroptical and NMR, data in structure assignment of natural products [15].

In the case of polyaurine B (**2**), in addition to the structure proposed on the basis of the obtained experimental data and literature reports (**2**, Figure 1), six possible alternative isomeric structures (**2a–2f**, Figure 4) were considered, quite compatible with the experimental NMR data.

For these six structures, the ^{13}C NMR chemical shift values were calculated using the GIAO method with the DFT technique. For this purpose, all the structures were previously subjected to an optimization of the geometry and energy optimization using DFT with the mPW1PW91/6-311+G(2d,p) functional and basis set combination [18–22]. The theoretical ^{13}C NMR chemical shift values predicted for **2a–2f** are reported in Table 2, in comparison to the experimental data obtained for the natural metabolite.

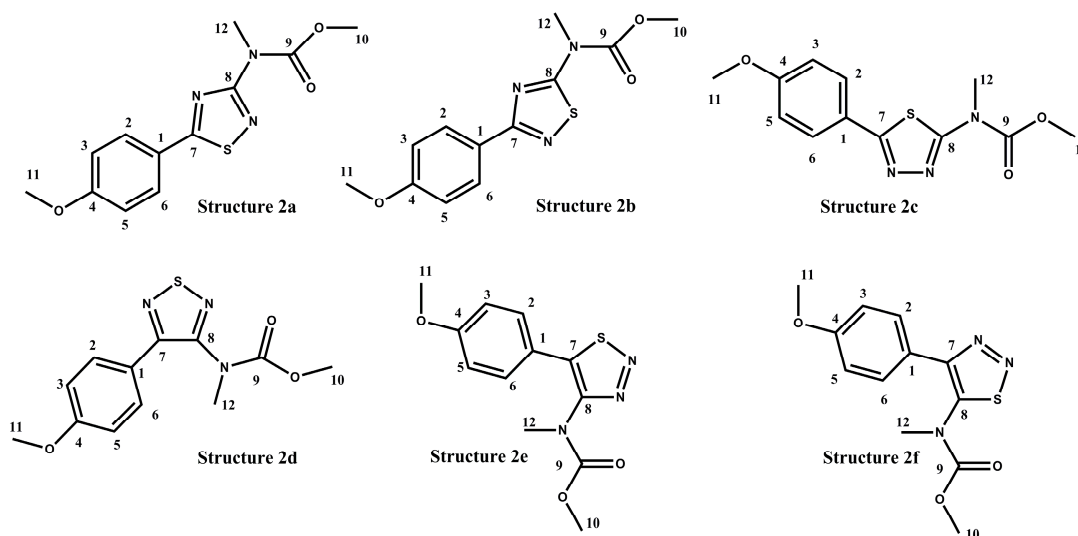


Figure 4. Isomeric alternative structures considered for polyaurine B (2).

Table 2. ^{13}C calculated and experimental NMR chemical shifts for structure 2a–2f. Chemical shift data here reported were produced using tetramethylsilane (TMS) as reference compound.

| - | Structure 2a | Structure 2b | Structure 2c | Structure 2d | Structure 2e | Structure 2f | Experimental Carbon |
|----|--------------|--------------|--------------|--------------|--------------|--------------|---------------------|
| 1 | 127.7 | 130.2 | 128.3 | 131.0 | 125.2 | 128.4 | 123.2 |
| 2 | 133.8 | 137.2 | 132.5 | 130.0 | 131.1 | 130.2 | 128.9 |
| 3 | 111.7 | 110.2 | 112.4 | 112.5 | 112.2 | 112.3 | 114.5 |
| 4 | 166.9 | 165.6 | 165.2 | 165.0 | 165.2 | 164.6 | 162.7 |
| 5 | 111.5 | 110.5 | 112.0 | 112.1 | 112.1 | 112.2 | 114.5 |
| 6 | 132.9 | 133.8 | 131.5 | 136.0 | 136.3 | 136.7 | 128.9 |
| 7 | 192.6 | 176.3 | 169.7 | 161.0 | 154.8 | 158.0 | 187.2 |
| 8 | 170.8 | 185.5 | 163.7 | 158.7 | 155.0 | 157.6 | 165.9 |
| 9 | 157.4 | 152.3 | 158.5 | 158.2 | 157.9 | 156.0 | 155.0 |
| 10 | 53.2 | 53.8 | 54.1 | 53.4 | 53.3 | 53.7 | 53.6 |
| 11 | 54.5 | 54.1 | 54.2 | 54.1 | 54.2 | 54.1 | 55.5 |
| 12 | 35.7 | 34.7 | 32.3 | 35.7 | 36.4 | 38.4 | 36.2 |

The analysis of the theoretical ^{13}C NMR data showed that the structure 2a was the correct isomer. The ^{13}C MAE (mean absolute errors) of 3.2 ppm and ^{13}C CMAE of 1.7 ppm (correct mean absolute errors) for the structure 2a was below 5 ppm in the ^{13}C NMR data, which is considered within the range of an acceptable DFT-NMR calculation for theoretical values. The theoretical ^{13}C NMR data was also analyzed through the DP4+ statistical analysis, which can be used to distinguish between constitutional isomers. The DP4+ analysis (Table 3) showed that ^{13}C NMR data were most consistent with the 2a structure (100% probability).

Table 3. The calculation results of structures 2a–2f with mean absolute errors (MAE) values and DP4+ probabilities.

| - | MAE Value (ppm) | | ^{13}C Data DP4+ Probability | | |
|--------------|---------------------|----------------------|---------------------------------------|---------|---------|
| | ^{13}C MAE | ^{13}C CMAE | sDP4+ | uDP4+ | DP4+ |
| Structure 2a | 3.2 | 1.7 | 100.00% | 100.00% | 100.00% |
| Structure 2b | 5.6 | 5.3 | 0.00% | 0.00% | 0.00% |
| Structure 2c | 3.9 | 4.2 | 0.00% | 0.00% | 0.00% |
| Structure 2d | 5.1 | 6.4 | 0.00% | 0.00% | 0.00% |
| Structure 2e | 5.6 | 7.3 | 0.00% | 0.00% | 0.00% |
| Structure 2f | 5.2 | 6.6 | 0.00% | 0.00% | 0.00% |

2.3. Biological Activities of Compounds 1 and 2

Polyaurines A (1) and B (2) were tested for their effects on the viability of NIH-3T3 mammalian cells and the *Schistosoma mansoni* parasite. Both compounds were not active and showed, in a dose-curve response, an IC_{50} higher than 100 μ M against both mammalian cells and larval stage (schistosomula) of *Schistosoma mansoni*.

The activity of polyaurine A was further investigated on adult *S. mansoni* pairs (Figure 5) with respect to polyaurine B considering the low available quantity for the latter.

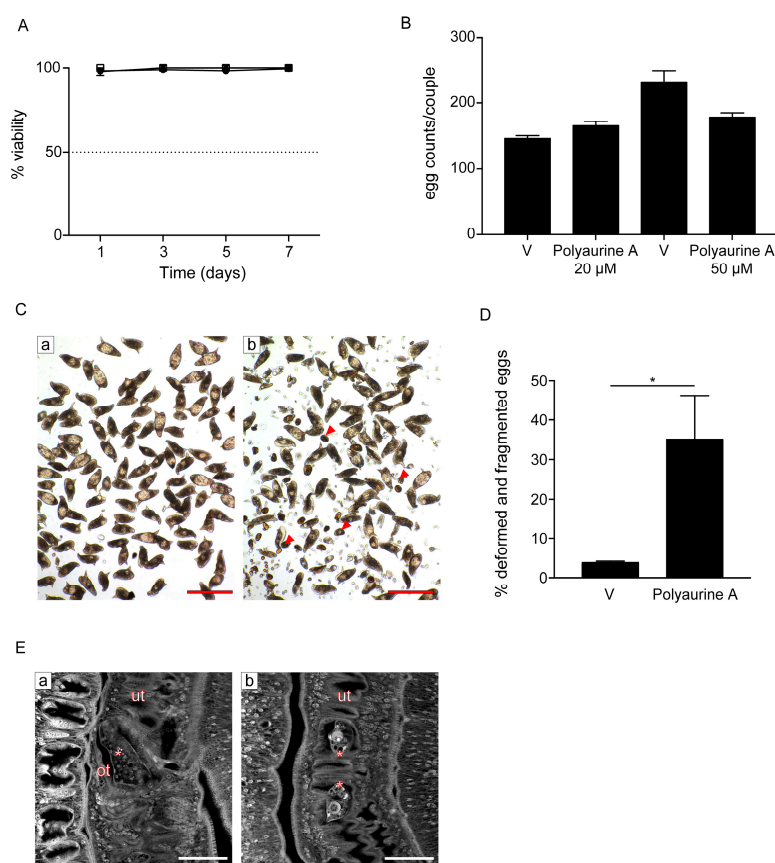


Figure 5. Effects of polyaurine A on *S. mansoni* adult parasites. **(A)** Adult pairs viability assays. Worm pairs were incubated with vehicle (DMSO) (circle), polyaurine A (1) 20 μ M (square), or 50 μ M (triangle), and viability is shown as the percentage of vehicle-treated samples indicated as 100%. The data shown represent the mean of three independent experiments \pm SEM. **(B)** Worm pairs were incubated with vehicle (V) or polyaurine A (1) at the indicated concentrations, and eggs were counted at 72 h. Egg counts were normalized to the number of worm couples. The data shown represent the mean of three independent experiments \pm SEM. **(C)** Representative microscopy images of *S. mansoni* eggs laid in vitro by worm pairs treated with vehicle (a) or 50 μ M of polyaurine A (1) (b). Red arrows indicate the deformed or fragmented eggs (b). Scale bars = 200 μ m. **(D)** Histograms represent the percentage of deformed and/or fragmented eggs counted at 72 h. Approximately 500 eggs were counted in 3 independent experiments (150–200 eggs/experiment). Asterisk in the figure indicates significant *t*-test *p*-value ($* p < 0.05$) relative to the comparison of 50 μ M of polyaurine A-treated samples with the vehicle V-treated ones. **(E)** Representative confocal scanning laser images of adult *S. mansoni* pairs treated for 72 h with vehicle or 50 μ M of polyaurine A. Eggs in the ootype (a, vehicle) or uterus (b, polyaurine A) are indicated by asterisks. Abbreviations: ot, ootype; ut, uterus. Scale-bars = 50 μ m. In all experiments, vehicle-treated parasites or eggs received the same amount of DMSO (in volume) as the polyaurine A (1)-treated ones.

Interestingly, while it did not impact parasite viability at both 20 and 50 μM during the seven days of observation (Figure 5A), it impaired egg production in vitro (Figure 5B–D). The total number of eggs laid by females upon treatment of *S. mansoni* pairs with both 20 and 50 μM of polyaurine A (**1**) or vehicle (DMSO) was similar (Figure 5B). However, some eggs laid in vitro by polyaurine A-treated parasites appeared deformed and several fragments of eggs were present in the plate dish, along with sperms and vitelline cells (Figure 5C). The number of deformed/fragmented eggs was quantified, and it resulted to be increased in the polyaurine A-treated samples in comparison to the DMSO-treated ones ($p < 0.05$) (Figure 5D). By carmine red-staining and confocal microscopy analyses, smaller size eggs were observed in the ootype and/or uterus of polyaurine A-treated parasites (Figure 5E). The eggs are crucial players in schistosomiasis for the maintenance of the parasite life-cycle, the definitive host tissue damage, and the development of the disease. Overall, these results indicate that polyaurine A is not cytotoxic on mammalian cells, but it is active on parasite egg production. Therefore, polyaurine A is an interesting bioactive natural molecule to be further investigated.

3. Materials and Methods

3.1. General Experimental Procedures

HRESIMS (positive mode) was performed on a Thermo LTQ Orbitrap XL mass spectrometer (Thermo-Fisher, San José, CA, USA). The spectra were recorded by infusion into the ESI source using MeOH as solvent. ^1H NMR (700 MHz and 500 MHz) and ^{13}C NMR (175 MHz and 125 MHz) spectra were recorded with an Agilent INOVA spectrometer (Agilent Technology, Cernusco sul Naviglio, Italy); chemical shifts were referenced to the residual solvent signal (CDCl_3 : $\delta_{\text{H}} = 7.26$, $\delta_{\text{C}} = 77.0$). Homonuclear ^1H connectivities were determined by COSY experiments. Two and three bond ^1H - ^{13}C connectivities were determined by gradient 2D HMBC experiments optimized for a 2,3J of 8 Hz. High performance liquid chromatography (HPLC) separation was achieved on a Knauer K-501 apparatus equipped with a Knauer K-2301 RI detector (LabService Analytica s.r.l., Anzola dell'Emilia, Italy).

3.2. Collection, Extraction, and Isolation

Specimens of *Polycarpa aurata* were collected along the coast of Siladen (Indonesia, $1^\circ 37' 41''$ N $124^\circ 48' 01''$ E) in the autumn of 2012. The identification of the organisms was carried out by Dr. Masteria Yunovilsa Putra. They were frozen immediately after collection and kept frozen until extraction. A voucher specimen is deposited at the Department of Pharmacy, University of Naples "Federico II", Naples, Italy.

Fresh thawed animals (39.8 g dry weight after extraction) were homogenized and extracted with MeOH (3×400 mL) and then with CHCl_3 (3×400 mL). Extracts were combined and concentrated in vacuo; the resulting aqueous residue was then partitioned giving EtOAc, *n*-BuOH, and aqueous extracts. The ethyl acetate-soluble material was chromatographed by MPLC over a silica gel column followed using an increasing gradient elution (100% *n*-hexane \rightarrow *n*-hexane:EtOAc 9:1 \rightarrow *n*-hexane:EtOAc 7:3 \rightarrow *n*-hexane:EtOAc 1:1 \rightarrow *n*-hexane:EtOAc 3:7 \rightarrow *n*-hexane:EtOAc 1:9 \rightarrow 100% EtOAc \rightarrow EtOAc:MeOH 9:1 \rightarrow 100% MeOH \rightarrow 100% CHCl_3) to yield eighteen fractions 1–18. The fractions (6–9) eluted with *n*-hexane:EtOAc 1:1 (*v/v*) were further purified by HPLC. Fraction 6 was chromatographed by HPLC Luna 3 μm Silica column, *n*-hexane:EtOAc (95:5) and yielded in pure form polyaurine A (**1**, t_{R} 9.2 min, 1.7 mg), polyaurine B (**2**, t_{R} 12.7 min, 0.5 mg), compound **3** (t_{R} 6.5 min, 0.2 mg), compound **4** (t_{R} 19.1 min, 0.6 mg), together with a mixture of compound **6** and **7** (t_{R} 20.6 min). HPLC on Luna 3 μm PFP column, MeOH:H₂O (75:25), allowed to separate into individual compounds, the latter mixture yielding compound **6** (t_{R} 8.3 min, 0.5 mg) and compound **7** (t_{R} 6.2 min, 0.7 mg) in the pure state. Fraction 7 was analyzed by HPLC on Luna 3 μm Silica column, *n*-hexane:EtOAc (85:15) afforded compound **8** (t_{R} 10.7 min, 0.5 mg) in pure state. Fraction 8 was analyzed by HPLC on Luna 3 μm Silica column, *n*-hexane:EtOAc (9:1), yielding a fraction mainly composed of **5** (t_{R} 22.4 min, 0.8 mg) which has been

further purified by HPLC on a RP-18 column (Luna 3 μ m PFP), eluting with MeOH:H₂O (7:3), thus affording compound **5** (t_R 5.1 min, 0.4 mg) as pure compound.

Polyaurine A (**1**): yellow powder; ¹H and ¹³C NMR data (CDCl₃) are reported in Table 1; 2D NMR data, Figures S4–S6; HRMS (ESI): m/z 266.1129 [M + H]⁺ (calcd. for C₁₂H₁₆O₄N₃: 266.1135); m/z 288.0948 [M + Na]⁺ (calcd. for C₁₂H₁₅O₄N₃Na: 288.0955) (Figure S1).

Polyaurine B (**2**): yellow powder; ¹H and ¹³C NMR data (CDCl₃) are reported in Table 1; 2D NMR data, Figures S10–S12; HRMS (ESI): m/z 280.0741 [M + H]⁺ (calcd. for C₁₂H₁₄O₃N₃S: 280.0750); m/z 302.0558 [M + Na]⁺ (calcd. for C₁₂H₁₃O₃N₃SNa: 302.0570) (Figure S7).

Compound **3**: white powder; ¹H NMR (CDCl₃) spectrum is reported in Supplementary Materials (Figure S14); HRMS (ESI): m/z 209.0810 [M + H]⁺ (calcd. for C₁₁H₁₃O₄: 209.0808); m/z 231.0630 [M + Na]⁺ (calcd. for C₁₁H₁₂O₄Na: 231.0628); m/z 231.0370 [M + K]⁺ (calcd. for C₁₁H₁₂O₄K: 247.0367) (Figure S13).

Compound **4**: white powder; ¹H NMR (CDCl₃) spectrum is reported in Supplementary Materials (Figure S16); HRMS (ESI): m/z 181.0491 [M + H]⁺ (calcd. for C₉H₉O₄: 181.0495); m/z 203.0309 [M + Na]⁺ (calcd. for C₉H₈O₄Na: 203.0315) (Figure S15).

Compound **5**: white powder; ¹H NMR (CDCl₃) spectrum is reported in Supplementary Materials (Figure S18); HRMS (ESI): m/z 236.0505 [M + H]⁺ (calcd. for C₁₀H₁₀N₃O₂S: 236.0488); m/z 258.0327 [M + Na]⁺ (calcd. for C₁₀H₉N₃O₂SNa: 258.0308) (Figure S17).

Compound **6**: yellow powder; $[\alpha]_D^{25}$ +33.5 (c 0.0002, CH₃OH); ¹H NMR (CDCl₃) spectrum is reported in Supplementary Materials (Figure S20); HRMS (ESI): m/z 289.0641 [M + Na]⁺ calcd. for C₁₂H₁₄N₂O₃SNa: 289.0617 (Figure S19).

Compound **7**: colourless oil; ¹H NMR (CDCl₃) spectrum is reported in Supplementary Materials (Figure S22); HRMS (ESI): m/z 195.0647 [M + H]⁺ (calcd. for C₁₀H₁₁O₄: 195.0652); m/z : 217.0465 [M + Na]⁺ (calcd. for C₁₀H₁₀O₄Na: 217.0471); m/z 233.0205 [M + K]⁺ (calcd. for C₁₀H₁₀O₄K⁺: 233.0211) (Figure S21).

Compound **8**: colourless oil; ¹H NMR (CDCl₃) spectrum is reported in Supplementary Materials (Figure S24); HRMS (ESI): m/z 194.0806 [M + H]⁺ (calcd. for C₁₀H₁₂NO₃: 194.0812); m/z 216.0625 [M + Na]⁺ (calcd. for C₁₀H₁₁NO₃Na: 216.0631) (Figure S23).

3.3. Biological Activity

3.3.1. Ethical Statement

Animal work was approved by the National Research Council, Institute of Cell Biology and Neurobiology animal welfare committee (OPBA) and by the competent authorities of the Italian Ministry of Health, DGSAF, Roma (authorizations no. 25/2014-PR and no. 336/2018-PR). All experiments were conducted in respect to the 3R rules according to the ethical and safety rules and guidelines for the use of animals in biomedical research provided by the relevant Italian law and European Union Directive (Italian Legislative Decree 26/2014 and 2010/63/EU) and the International Guiding Principles for Biomedical Research involving animals (Council for the International Organizations of Medical Sciences, Geneva, Switzerland).

3.3.2. Maintenance of the *S. mansoni* Life-Cycle

A Puerto Rican strain of *S. mansoni* was maintained in albino *Biomphalaria glabrata*, as the intermediate host, and ICR (CD-1) outbred female mice as the definitive host as previously described [23]. Female 7- to 8-week-old mice (Envigo, Udine, Italy) were infected with 150–200 double sex *S. mansoni* cercariae by the tail immersion technique.

3.3.3. Preparation of Parasites, Viability Assays, and Eggs Analysis

Schistosomula were prepared by mechanical transformation of cercariae, and adult worm pairs were isolated by reversed perfusion of the hepatic portal system and mesenteric veins of 7–8 weeks post-infection. The protocols for the parasite preparation have been previously reported [23]. The schistosomula ATP-based assay was performed in 96-wells/cell culture black microplate (Greiner Bio-One S.r.l, Roma, Italy, #655090) with the CellTiterGlo (CTG) (Promega, Madison, WI, USA) as previously described but using 150–200 schistosomula/well and 50 μ L of CTG [23]. The luminescence signal was measured with a Varioskan Lux and the Skanit software (ThermoFisher Scientific, Waltham, MA, USA). The percentage of dead schistosomula for each compound was calculated as the ATP reduction against vehicle and gambogic acid (50 μ M) used, respectively, as negative (0%) and positive control (100%). For the adult worm parasites assays, 5 adult male–female pairs were cultured in tissue culture medium. Vehicle (DMSO) or polyaurine A were added to the parasite at 20 and 50 μ M concentrations only once 24 h upon parasite isolation from infected mice and observed for seven days. A survival score was assigned daily based on phenotype (plate-attached, movement, color, gut peristalsis, tegument damage, male–female pairing) under a MZ12 stereomicroscope (Leica Microsystems, Mannheim, Germany) as previously reported [23]. The percentage severity score (viability) was assigned in three independent experiments, relative to DMSO. For in vitro eggs laying, 5 worm adult pairs were incubated with DMSO or polyaurine A (1), the number of eggs was counted at 72 hours, and normalized to parasite pairs. Images of eggs were recorded with a BX41 microscope and a brightfield objective 10 \times served by a SPOT RT 220-3 Diagnostic Instrument Inc camera (Olympus, Waltham, MA, USA).

3.3.4. Confocal Laser Scanning Microscopy Analysis

Carmine-red staining was performed on parasite pairs as previously described [24]. Images were taken on a FV1200 confocal laser-scanning microscope using an UPlanFLN 40 \times immersion oil objective (NA = 1.30) and a multiline argon laser at 488 nm as the excitation source (Olympus, Waltham, MA, USA). The images were collected as a single stack.

3.3.5. Viability Mammalian Cell Assay

NIH-3T3 mouse embryonic fibroblasts, plated in 96-well plates at day 0 were treated with increasing concentrations of compound (0.4×10^4 cells/well) 1 or 2 (from 0.390 up to 100 μ M) in complete tissue culture medium and cultured for 72 h at 37 $^{\circ}$ C in 5% CO₂. MTT was used at 1 mg/mL and formazan crystals were solubilized with DMSO. The plates were analyzed with the Varioskan Lux and the Skanit software (Thermo Fisher Scientific, Waltham, MA, USA) at 570 nm and 630 nm.

3.3.6. Statistical Analysis

All statistical tests were performed using GraphPad Prism v.6.0c software. All viability data are shown as the mean \pm standard error of the mean (SEM). Differences in the number of abnormal/fragmented eggs were analyzed by Student's *t*-test. *P*-values \leq 0.05 was considered to be statistically significant.

4. Conclusions

1,2,4-Thiadiazole alkaloids are rarely found in natural products and, to our knowledge, polyaurine B represents the first example of a marine natural 3-(*N*-methyl-methylcarbamate) substituted 1,2,4-thiadiazole alkaloid. Its structure was elucidated at first by spectroscopic means and by comparing its spectral feature to those reported in the literature for the few reference compounds [5,12–14]. Further support to the proposed (5-(4-methoxyphenyl)-1,2,4-thiadiazol-3-yl)(methyl)carbamate structure was gained by the quantum mechanical calculation of its ¹³C NMR chemical shifts profile and application of DP4+ statistical analysis, a kind of approach which is becoming an important tool for structure

elucidation of natural products. Definitely, polyaurines A and B are not cytotoxic on mammalian NIH-3T3 cells and on different stages of *S. mansoni*, although polyaurine A, interestingly, impairs egg production in vitro representing, therefore, a natural molecule with interesting biological properties. The egg phenotype could be further investigated by electron microscopy analyses and comparative proteomic studies in order to identify polyaurine A-targets.

Supplementary Materials: The following are available online at <http://www.mdpi.com/1660-3397/17/5/278/s1>, Figure S1. HRESIMS spectrum of polyaurine A (1); Figure S2. ¹H NMR spectrum of polyaurine A (1) in CDCl₃; Figure S3. ¹³C NMR spectrum of polyaurine A (1) in CDCl₃; Figure S4. HSQC spectrum of polyaurine A (1) in CDCl₃; Figure S5. COSY spectrum of polyaurine A (1) in CDCl₃; Figure S6. HMBC spectrum of polyaurine A (1) in CDCl₃; Figure S7. HRESI-MS spectrum of polyaurine B (2); Figure S8. ¹H NMR spectrum of polyaurine B (2) in CDCl₃; Figure S9. ¹³C NMR spectrum of polyaurine B (2) in CDCl₃; Figure S10. HSQC spectrum of polyaurine B (2) in CDCl₃; Figure S11. COSY spectrum of polyaurine B (2) in CDCl₃; Figure S12. HMBC spectrum of polyaurine B (2) in CDCl₃; Figure S13. HRESI-MS spectrum of compound 3; Figure S14. ¹H NMR spectrum of compound 3 in CDCl₃; Figure S15. HRESI-MS spectrum of compound 4; Figure S16. ¹H NMR spectrum of compound 4 in CDCl₃; Figure S17. HRESI-MS spectrum of compound 5; Figure S18. ¹H NMR spectrum of compound 5 in CDCl₃; Figure S19. HRESI-MS spectrum of compound 6; Figure S20. ¹H NMR spectrum of compound 6 in CDCl₃; Figure S21. HRESI-MS spectrum of compound 7; Figure S22. ¹H NMR spectrum of compound 7 in CDCl₃; Figure S23. HRESI-MS spectrum of compound 8; Figure S24. ¹H NMR spectrum of compound 8 in CDCl₃.

Author Contributions: Conceptualization, C.I. and M.M.; data curation, M.C., C.I., P.L., A.A., M.Y.P., R.G., G.R. and M.M.; formal analysis, M.C., R.G. and G.R.; funding acquisition, G.R. and M.M.; investigation, M.C. and C.I.; methodology, M.C., P.L. and R.G.; resources, M.Y.P.; writing—original draft, C.I. and M.M.; writing—review and editing, M.C., C.I., P.L., A.A., M.Y.P., R.G., G.R. and M.M.

Funding: This work was supported by Ministero dell’Istruzione, dell’ Università e della Ricerca (MIUR), PRIN Projects 2010C2LKKJ_006; 20154JRJPP_004 and by a grant from Regione Campania-POR Campania FESR 2014/2020 “Combattere la resistenza tumorale: piattaforma integrata multidisciplinare per un approccio tecnologico innovativo alle oncoterapie-Campania Oncoterapie” (Project N. B61G18000470007).

Acknowledgments: We are grateful to Alessandra Guidi and Fulvio Saccoccia of the Institute of Cell Biology and Neurobiology, National Research Council, for their support in the *S. mansoni* life cycle maintenance and for critical discussions. Special thanks to Stefania Colantoni for mouse husbandry.

Conflicts of Interest: The authors declare no conflict of interest.

References

1. Davison, E.K.; Sperry, J. Natural Products with Heteroatom-Rich Ring Systems. *J. Nat. Prod.* **2017**, *80*, 3060–3079. [[CrossRef](#)]
2. Abas, S.A.; Hossain, M.B.; van der Helm, D.; Schmitz, F.J.; Laney, M.; Cabuslay, R.; Schatzman, R.C. Alkaloids from the Tunicate *Polycarpa aurata* from Chuuk Atoll. *J. Org. Chem.* **1996**, *61*, 2709–2712. [[CrossRef](#)]
3. Lindquist, N.; Fenical, W. Polycarpamines A-E, antifungal disulfides from the marine ascidian *Polycarpa auzata*. *Tetrahedron Lett.* **1990**, *31*, 2389–2392. [[CrossRef](#)]
4. Wang, W.; Oda, T.; Fujita, A.; Mangindaan, R.E.P.; Nakazawa, T.; Ukai, K.; Kobayashi, H.; Namikoshi, M. Three new sulfur-containing alkaloids, polycarpaurines A, B, and C, from an Indonesian ascidian *Polycarpa aurata*. *Tetrahedron* **2007**, *63*, 409–412. [[CrossRef](#)]
5. Pham, C.; Weber, H.; Hartmann, R.; Wray, V.; Lin, W.; Lai, D.; Proksch, P. New Cytotoxic 1,2,4-Thiadiazole Alkaloids from the Ascidian *Polycarpa aurata*. *Org. Lett.* **2013**, *15*, 2230–2233. [[CrossRef](#)]
6. Wessels, M.; König, G.M.; Wright, A.D. New 4-Methoxybenzoyl Derivatives from the Ascidian *Polycarpa aurata*. *J. Nat. Prod.* **2001**, *64*, 1556–1558. [[CrossRef](#)] [[PubMed](#)]
7. Kang, H.; Fenical, W. Polycarpinedihydrochloride: A cytotoxic dimeric disulfide alkaloid from the Indian ocean ascidian *Polycarpa clavata*. *Tetrahedron Lett.* **1996**, *37*, 2369–2372. [[CrossRef](#)]
8. Popov, A.M.; Novikov, V.L.; Radchenko, O.S.; Elyakov, G.B. The cytotoxic and antitumor activities of the imidazole alkaloid polycarpin from the ascidian *Polycarpa aurata* and its synthetic analogues. *Dokl. Biochem. Biophys.* **2002**, *385*, 213–218. [[CrossRef](#)] [[PubMed](#)]

9. Fedorov, S.N.; Bode, A.M.; Stonik, V.A.; Gorshkova, I.A.; Schmid, P.C.; Radchenko, O.S.; Berdyshev, E.V.; Dong, Z. Marine Alkaloid Polycarpine and Its Synthetic Derivative Dimethylpolycarpine Induce Apoptosis in JB6 Cells Through p53- and Caspase 3-Dependent Pathways. *Pharm. Res.* **2004**, *21*, 2307–2319. [[CrossRef](#)] [[PubMed](#)]
10. Colley, D.G.; Bustinduy, A.L.; Secor, W.E.; King, C.H. Human schistosomiasis. *Lancet* **2014**, *383*, 2253–2264. [[CrossRef](#)]
11. Cioli, D.; Pica-Mattocchia, L.; Basso, A.; Guidi, A. Schistosomiasis control: Praziquantel forever? *Mol. Biochem. Parasitol.* **2014**, *195*, 23–29. [[CrossRef](#)]
12. Heitz, S.; Durgeat, M.; Guyot, M.; Brassy, C.; Bachet, B. Nouveau derive indolique du thiadiazole-1,2,4, isole d'un tunicier (*Dendrodoa grossularia*). *Tetrahedron Lett.* **1980**, *21*, 1457–1458. [[CrossRef](#)]
13. Chen, M.; Lin, S.; Li, L.; Zhu, C.; Wang, X.; Wang, Y.; Jiang, B.; Wang, S.; Li, Y.; Jiang, J.; et al. Enantiomers of an Indole Alkaloid Containing Unusual Dihydrothiopyran and 1,2,4-Thiadiazole Rings from the Root of *Isatis indigotica*. *Org. Lett.* **2012**, *14*, 5668–5671. [[CrossRef](#)] [[PubMed](#)]
14. Yang, Z.; Huang, N.; Xu, B.; Huang, W.; Xie, T.; Cheng, F.; Zou, K. Cytotoxic 1,3-Thiazole and 1,2,4-Thiadiazole Alkaloids from *Penicillium oxalicum*: Structural Elucidation and Total Synthesis. *Molecules* **2016**, *21*, 232. [[CrossRef](#)] [[PubMed](#)]
15. Davison, E.K.; Sperry, J. Synthesis of the 1,2,4-thiadiazole alkaloids polycarpathamines A and B. *Org. Chem. Front.* **2016**, *3*, 38–42. [[CrossRef](#)]
16. Pätzel, M.; Liebscher, J.; Andreae, S.; Schmitz, E. Ring Transformations of Semicyclic 1,3-Dicarbonyl Heteroanalogs; IV. Synthesis of 3-(ω -Aminoalkyl)-1,2,4-thiadiazoles by Ring Transformation Reaction of Semicyclic Thioacylamidines with 3,3-Pentamethyleneoxaziridine. *Synthesis* **1990**, *11*, 1071–1073. [[CrossRef](#)]
17. Hogan, I.T.; Sainsbury, M. The synthesis of dendrodoine, 5-[3-(N,N-dimethylamino-1,2,4-thiadiazolyl)]-3-indolylmethanone, a metabolite of the marine tunicate *Dendrodoa grossularia*. *Tetrahedron* **1984**, *40*, 681–682. [[CrossRef](#)]
18. Imperatore, C.; Luciano, P.; Aiello, A.; Vitalone, R.; Irace, C.; Santamaria, R.; Li, J.; Guo, Y.-W.; Menna, M. Structure and Configuration of Phosphoeleganin, a Protein Tyrosine Phosphatase 1B Inhibitor from the Mediterranean Ascidian *Sidnyum elegans*. *J. Nat. Prod.* **2016**, *79*, 1144–1148. [[CrossRef](#)]
19. Luciano, P.; Imperatore, C.; Senese, M.; Aiello, A.; Casertano, M.; Guo, Y.; Menna, M. Assignment of the Absolute Configuration of Phosphoeleganin via Synthesis of Model Compounds. *J. Nat. Prod.* **2017**, *80*, 2118–2123. [[CrossRef](#)]
20. Chianese, G.; Yu, H.-B.; Yang, F.; Sirignano, C.; Luciano, P.; Han, B.-N.; Khan, S.; Lin, H.-W.; Tagliatela-Scafati, O. PPAR Modulating Polyketides from a Chinese *Plakortis simplex* and Clues on the Origin of Their Chemodiversity. *J. Org. Chem.* **2016**, *81*, 5135–5143. [[CrossRef](#)]
21. Menna, M.; Aiello, A.; D'Aniello, F.; Fattorusso, E.; Imperatore, C.; Luciano, P.; Vitalone, R. Further investigation of the Mediterranean sponge *Axinella polypoides*: Isolation of a new cyclonucleoside and a new betaine. *Mar. Drugs* **2012**, *10*, 2509–2518. [[CrossRef](#)]
22. Menna, M.; Imperatore, C.; Mangoni, A.; Della Sala, G.; Tagliatela-Scafati, O. Challenges in the configuration assignment of natural products. A case-selective perspective. *Nat. Prod. Rep.* **2019**, *36*, 476–489. [[CrossRef](#)] [[PubMed](#)]
23. Lalli, C.; Guidi, A.; Gennari, N.; Altamura, S.; Bresciani, A.; Ruberti, G. Development and validation of a luminescence-based, medium-throughput assay for drug screening in *Schistosoma mansoni*. *PLoS Negl. Trop. Dis.* **2015**, *9*, e0003484. [[CrossRef](#)]
24. Guidi, A.; Lalli, C.; Perlas, E.; Bolasco, G.; Nibbio, M.; Monteagudo, E.; Bresciani, M.; Ruberti, G. Discovery and Characterization of novel anti-schistosomal properties of the anti-anginal drug, perhexiline and its impact on *Schistosoma mansoni* male and female reproductive systems. *PLoS Negl. Trop. Dis.* **2016**, *10*, e0004928. [[CrossRef](#)] [[PubMed](#)]

